

SnO₂ assembly. Any opinions, findings, and conclusions or recommendations expressed in this paper are those of the authors and do not necessarily reflect the view of the National Science Foundation.

REFERENCES

- [1] A. Bezryadin and C. Dekker, "Nanofabrication of electrodes with sub-5 nm spacing for transport experiments on single molecules and metal clusters," *J. Vac. Sci. Technol. B*, vol. 15, pp. 793–799, 1997.
- [2] C. Baur, A. Bugacov, and B. Koel, "Nanoparticle manipulation by mechanical pushing: Underlying phenomena and real-time monitoring," *Nanotechnol.*, vol. 9, pp. 360–364, 1998.
- [3] T. Vargo and J. Calvert, "Patterned polymer multilayer fabrication by controlled adhesion of polyelectrolytes to plasma-modified fluoropolymer surfaces," *Supramol. Sci.*, vol. 2, pp. 169–174, 1995.
- [4] A. Rogach, A. Susha, F. Caruso, G. Sukhorukov, A. Kornowski, S. Kershaw, H. Möhwald, A. Eychmüller, and H. Weller, "Nano- and microengineering: Three-dimensional colloidal photonic crystals prepared from submicrometer-sized polystyrene latex spheres pre-coated with luminescent polyelectrolyte/nanocrystal shells," *Adv. Mater. Process.*, vol. 12, pp. 333–337, 2000.
- [5] G. Ozin and S. Yang, "The race for the photonic chip, opal-patterned chips," *Adv. Funct. Mater.*, vol. 11, pp. 1–10, 2001.
- [6] M. Onoda, H. Nakayama, T. Yamaue, K. Tada, and K. Yoshino, "Properties of light-emitting diodes fabricated from self-assembled multilayer heterostructures of poly (P-pyridyl vinylene)," *Jpn. J. Appl. Phys.*, vol. 36, pp. 5322–5328, 1997.
- [7] D. Yoo, J. K. Lee, and M. F. Rubner, "Investigations of new self-assembled multilayer thin films based on alternately adsorbed layers of polyelectrolytes and functional dye molecules," in *Proc. Mater. Res. Soc. Symp.*, vol. 413, 1996, pp. 395–400.
- [8] G. Chen, "Particularities of heat conduction in nanostructures," *J. Nanoparticle Res.*, vol. 2, pp. 199–204, 2000.
- [9] Y. Takeda, V. Gritsyna, N. Umeda, and C. Lee, "Optical properties of nanoparticle composites in insulators by high-flux 60 keV Cu implantation," *Nuclear Instrum. Methods Phys. Res. B, Beam Interact. Mater. At.*, vol. 148, pp. 1029–1034, 1999.
- [10] H. Doumanidis, "The nanomanufacturing programme at the national science foundation," *Nanotechnol.*, vol. 13, pp. 248–252, 2002.
- [11] G. Decher, "Fuzzy nanoassemblies: Toward layered polymeric multicomposites," *Sci.*, vol. 227, pp. 1232–1237, 1997.
- [12] Y. Lvov, K. K. Ariga, K. Ichinose, and T. Kunitake, "Alternate assembly of ordered multilayers of SiO₂ and other nanoparticles and polyions," *Langmuir*, vol. 13, pp. 6195–6203, 1997.
- [13] A. Rosidian, Y. Liu, and R. Claus, "Ionic self-assembly of ultrahard ZrO₂/polymernanocomposite thin films," *Adv. Mater.*, vol. 10, pp. 1087–1091, 1998.
- [14] S. Joly, R. Kane, L. Radzilowski, T. Wang, A. Wu, R. Cohen, E. Thomas, and M. Rubner, "Multilayer nanoreactors for metallic and semiconducting particles," *Langmuir*, vol. 16, pp. 1354–1359, 2000.
- [15] A. Mamedov, A. Belov, M. Giersig, N. Mamedova, and N. Kotov, "Nanorainbow: Graded semiconductor films from quantum dots," *J. Amer. Chem. Soc.*, vol. 123, pp. 7738–7739, 2001.
- [16] C. Lesser, M. Gao, and S. Kirstein, "Highly luminescent thin films from alternating deposition of CdTe nano-particles and polycations," *Mater. Sci. Eng.*, vol. C 8–9, pp. 159–162, 1999.
- [17] T. Cassagneau, J. Fendler, and T. Mallouk, "Optical and electrical characterizations of ultrathin films self-assembled from 11-Aminoundecanoic acid capped TiO₂ nanoparticles and polyallylamine hydrochloride," *Langmuir*, vol. 16, pp. 241–246, 2000.
- [18] X. Lin, R. Parthasarathy, and H. Jaeger, "Direct patterning of self-assembled nanocrystal monolayer by electron beam lithography," *Appl. Phys. Lett.*, vol. 78, pp. 1915–1917, 2001.
- [19] G. Kenausis, I. Janos, and D. Elbert, "Poly(L-lysine)-g-poly(Ethylene glycol) layers on metal oxide surfaces: Attachment mechanism and effects of polymer architecture on resistance to protein adsorption," *J. Phys. Chem.*, vol. 104, pp. 3298–3309, 2000.
- [20] C. Bulthaupt, E. Wilhelm, and B. Hubert, "All additive fabrication of inorganic logic elements by liquid embossing," *Appl. Phys. Lett.*, vol. 79, pp. 1525–1527, 2001.
- [21] L. Brott, R. Naik, and D. Pikas, "Ultrafast holographic nanopatterning of biocatalytically formed silica," *Nature*, vol. 413, pp. 291–293, 2001.

- [22] T. Vossmeier, S. Jia, E. DeIonno, M. Diehl, and S. Kim, "Combinatorial approaches toward patterning nanocrystals," *J. Appl. Phys.*, vol. 84, pp. 3664–3670, 1998.
- [23] C. L. Haynes and R. P. Van Duyne, "Nanosphere lithography: A versatile nanofabrication tool for studies of size-dependent nanoparticle optics," *J. Phys. Chem.*, vol. 105, pp. 5599–5611, 2001.
- [24] S. Yang and M. Rubner, "Micropatterning of polymer thin films using pH-sensitive and crosslinkable hydrogen-bonded polyelectrolyte multilayers," *J. Amer. Chem. Soc.*, vol. 124, pp. 2100–2101, 2002.
- [25] X. Jiang and P. Hammond, "Selective deposition in layer-by-layer assembly: Functional graft copolymers as molecular templates," *Langmuir*, vol. 16, pp. 8501–8509, 2000.
- [26] H. Zheng, I. Lee, M. F. Rubner, and P. T. Hammond, "Controlled cluster size in patterned particle arrays via directed adsorption on confined surfaces," *Adv. Mater. Process.*, vol. 14, pp. 569–572, 2002.
- [27] F. Hua, Y. Lvov, and T. Cui, "Spatial patterning of colloidal nanoparticle-based thin film by a combinative technique of layer-by-layer self-assembly and lithography," *J. Nanosci. Nanotechnol.*, vol. 2, pp. 357–361, 2002.
- [28] F. Hua, J. Shi, Y. Lvov, and T. Cui, "Patterning of layer-by-layer self-assembled multiple types of nanoparticle thin films by lithographic technique," *Nano Lett.*, vol. 2, pp. 1219–1222, 2002.
- [29] —, "Fabrication and characterization of metal-oxide-semiconductor capacitor based on layer-by-layer self-assembled thin films," *Nanotechnology*, vol. 14, pp. 403–457, 2003.
- [30] C. Tedeschi, H. Möhwald, and S. Kirstein, "Polarity of layer-by-layer deposited polyelectrolyte films as determined by pyrene fluorescence," *J. Amer. Chem. Soc.*, vol. 123, pp. 954–960, 2001.
- [31] G. Sauerbrey, "Verwendung von schwingquarzen zur Wägung d'Äunnen schichten und zur Mikrowägung," *Z. Phys.*, vol. 155, pp. 206–212, 1959.
- [32] E. Yang, *Microelectronic Devices*. New York: McGraw-Hill, 1988.

Diffusion Capacitance and Laser Diodes

John Strologas and Karl Hess

Abstract—The well-known diffusion capacitance is critical in determining the modulation response of p–n junctions and particularly of laser diodes. In this brief, we investigate the diffusion capacitance of a diode, as a function of the physical length of the diode and the carrier lifetimes in the narrow active region. We show that diode length and lifetime together, and not just the lifetime (which is well known), determine the bandwidth of the diode.

Index Terms—Carrier lifetime, depletion capacitance, diffusion capacitance, diode length, laser diode, modulation response.

I. INTRODUCTION

In this brief, we consider a symmetric one-dimensional (1-D) diode extending from $x = -L$ to $x = L$, where the negative x region is the

Manuscript received July 9, 2003; revised November 13, 2003. This work was supported in part by the United States Department of Energy under Grant DE-FG02-91ER-40677 and the Army Research Office under Grant DAAG 55-09-1-0306. The review of this brief was arranged by Editor P. Bhattacharya.

J. Strologas was with the Physics Department and Electrical and Computer Engineering Department, University of Illinois at Urbana-Champaign, Urbana, IL 61801 USA. He is now with the Fermi National Accelerator Laboratory, Batavia, IL 60510 USA, and also with the Physics and Astronomy Department of the University of New Mexico, Albuquerque, NM 87131 USA (e-mail: strolog@fnal.gov).

K. Hess is with the Electrical and Computer Engineering Department and the Beckman Institute, University of Illinois, Urbana-Champaign, IL 61801 USA. Digital Object Identifier 10.1109/TED.2003.822345

p-region, with an abrupt junction at $x = 0$. The design of the diode and its material parameters are chosen in a generic and standard way, except that at the junction we include a narrow region of very short carrier lifetimes, thus emulating a situation as it is encountered in laser diodes. Our results are therefore expected to be quite general and reflect some of the essential behavior of laser diodes. The main point that we show is that the high frequency response of a p–n junction and its bandwidth depends in a complex way on both the diode length and carrier lifetimes and not just on the lifetimes, as it is usually assumed in textbooks. To show this, we compute the diode capacitance numerically using a commercial simulator.

The diffusion capacitance of the diode is defined as¹

$$C_{\text{diff}} = \int_0^L 2e \frac{\partial p(x, V)}{\partial V} dx \quad (1)$$

and its depletion capacitance as

$$C_{\text{dep}} = \int_0^L e \frac{\partial(n(x, V) - p(x, V))}{\partial V} dx \quad (2)$$

where $p(x, V)$ and $n(x, V)$ are the hole and electron densities as a function of the spatial position x along the diode and the external forward bias V , and e is the electron charge [1], [2]. Notice that the diffusion capacitance is related to the minority carrier density (in this expression, the density of holes in the n-region). These two capacitances are connected in parallel and the total capacitance that affects the frequency response of the diode is given by their sum.

At the typical operation point of light emitting diodes (forward voltage equal to E_g/e [3], where E_g is the semiconductor energy gap) the diffusion capacitance is typically large and represents the major factor for the bandwidth. In fact, most standard texts derive an exponentially increasing diffusion capacitance even for long diodes ($L \gg \sqrt{D\tau}$, where D is the diffusion constant and τ is the lifetime of the carriers). It has been shown, however, that very long diodes with low carrier lifetimes may have a very low diffusion capacitance and therefore a large bandwidth [4].

To minimize C_{diff} , in order to increase the speed of the diode, the minority carriers should recombine before they reach the contacts and their charge should thus not be reclaimable. This situation is common in edge emitting laser diodes. These diodes are relatively long, and the carrier lifetime τ in their active region around the junction is extremely short due to stimulated emission. Vertical cavity surface emitting laser diodes (VCSELs) are shorter with their length determined by cavity and Bragg-reflectors.

In this brief, we present simulation results for the diffusion capacitance of p–n junction diodes (having the typical lifetime of laser diodes) as a function of length L and lifetime τ in the active region [5]. We arrive at iso-diffusion-capacitance curves, which determine which combinations of L and τ result in the same diffusion capacitance at a given operation point. We also discuss specific limits where the diffusion capacitance is significantly larger than the depletion capacitance and where these diffusion iso-capacitance curves are actually iso-curves for the modulation response. These curves are then useful to estimate the influence of diffusion capacitance on diode (and particularly laser diode) modulation response. To achieve these goals we design and simulate many diodes with different L and τ parameters, using the ISE-TCAD software [6]. To be as general as possible, we consider only the carrier lifetimes in the active region, without concentrating on the particular details and possible quantum structure of the active region.

¹If the “ U_s -term” [1] is taken into account, the factor of 2 can be ignored. This does not significantly change our results in logarithmic scale.

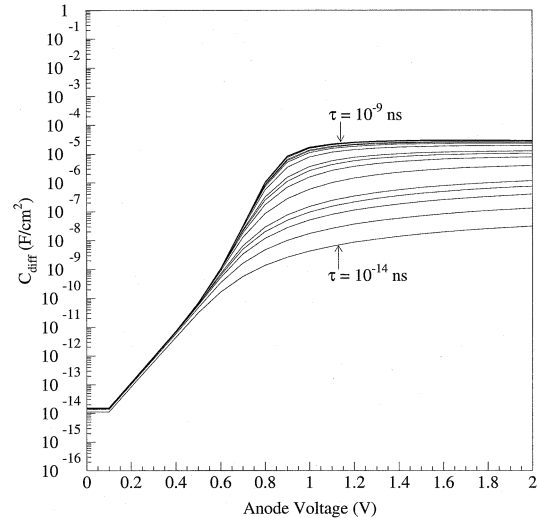


Fig. 1. Diffusion capacitance as a function of the anode voltage, for a diode with $L = 5 \mu\text{m}$ and 21 values of τ ranging from 10^{-14} to 10^{-9} s.

II. DIODE SIMULATION

To simulate the diode, we design a regular symmetric 1–D diode using the ISE-TCAD software, and we subsequently reduce the lifetimes of the carriers in a region around the junction. The carriers’ lifetime outside the active region is set to 10^{-9} s and their lifetime in the active region (τ) is varied from 10^{-14} to 10^{-9} s.² We simulate symmetric generic diodes by selecting physical characteristics (for band gap, etc.) that lie between the values of Si and GaAs. The half-length of the diodes (distance from the anode or cathode to the junction) is varied from 5 nm to 1 mm.³ The laser active region is set to be 5 nm around the junction. For every diode, we vary the applied external forward bias from 0 to twice the value of E_g/e . We simulated different values for E_g and we found that the only effect was a respective horizontal shift in the plots of the capacitances as a function of the externally applied forward bias. We thus present the results only for $E_g = 1$ eV.

Figs. 1 and 2 show the diffusion and depletion capacitance respectively, for $L = 5 \mu\text{m}$ and the 21 selections of τ , ranging from 10^{-14} to 10^{-9} s. According to these Figures, at low bias, the depletion capacitance is greater than the diffusion capacitance. The minority carriers do not reach the contacts, their charge is not reclaimable, and they do not contribute to the diffusion capacitance. As the voltage increases, the depletion capacitance increases, since the depletion region width decreases. At voltage close to the built-in voltage, the depletion capacitance reaches its maximum, the diffusion capacitance is no longer negligible and begins increasing. At higher voltage, the depletion capacitance decreases, as the diode is depleted and there is no charge stored in the junction to vary with anode voltage, while the diffusion capacitance keeps increasing. At bias equal to E_g/e (1 V in our case), which is close to the operational bias of the laser diodes, the diffusion capacitance prevails. It is important to note that the diffusion capacitance is small compared to the depletion capacitance, if the carrier lifetime τ in the lasing region is extremely low. This is because only few minority carriers reach the contacts of the diode, even if the anode voltage is high. On the other hand, for larger values of τ , and for anode voltages equal to the operational bias of the device, the diffusion capacitance is dominant and represents the main factor that determines the modulation response of the diode.

²We used 21 τ values, following the expression $\tau = T \times 10^k$ s, where $T = 1, 2.5, 5,$ and 7.5 and $k = -14$ to -9 .

³We used 20 L values: 0.005, 0.01, 0.02, 0.05, 0.1, 0.2, 0.5, 1, 2, 5, 10, 20, 40, 60, 80, 100, 200, 500, 800, and 1000 μm .

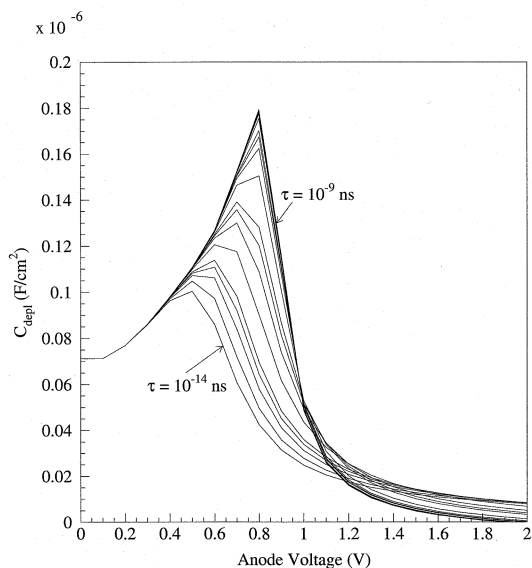


Fig. 2. Depletion capacitance as a function of the anode voltage, for a diode with $L = 5 \mu\text{m}$ and 21 values of τ ranging from 10^{-14} to 10^{-9} s.

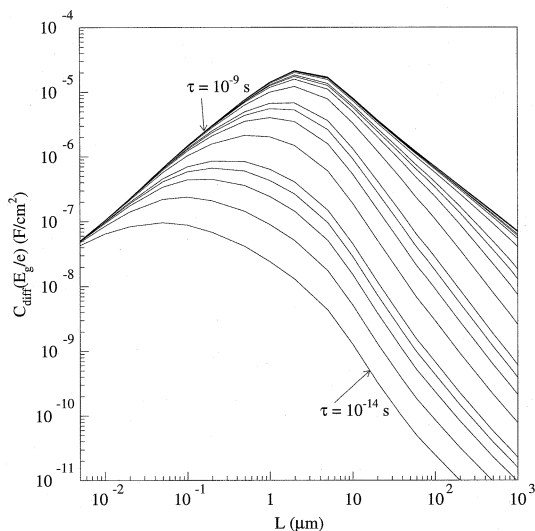


Fig. 3. $C_{\text{diff}}(E_g/e)$ as a function of L for 21 values of τ ranging from 10^{-14} to 10^{-9} s.

A FORTRAN analysis program receives the file containing the diffusion capacitance voltage distributions for all simulated diodes, and extracts the diffusion capacitance $C_{\text{diff}}(E_g/e)$ for every (L, τ) combination. It also computes the iso- $C_{\text{diff}}(E_g/e)$ curves of the values of L and τ that result in the same $C_{\text{diff}}(E_g/e)$. By selecting combinations of L and τ that correspond to low $C_{\text{diff}}(E_g/e)$, one can improve the bandwidth of the diode considerably. Fig. 3 shows $C_{\text{diff}}(E_g/e)$ as a function of L for the 21 values of τ , ranging from 10^{-14} s to 10^{-9} s, and Fig. 4 shows $C_{\text{diff}}(E_g/e)$ as a function of τ for the 20 values of L , ranging from 5 nm to 1 mm.

According to Fig. 3, there is an increase of $C_{\text{diff}}(E_g/e)$ as a function of L , for low values of L . For longer diodes, the diffusion capacitance decreases with L . The reason for this behavior are two counteracting phenomena that contribute to the diffusion capacitance as L increases. On one hand, the available charge increases (this increases the diffusion capacitance), and at the same time, the probability that the minority carriers reach the contact decreases (this decreases the diffusion capacitance). For very low τ the second phenomenon predominates, whereas at high τ , the first one prevails up to a critical value of L .

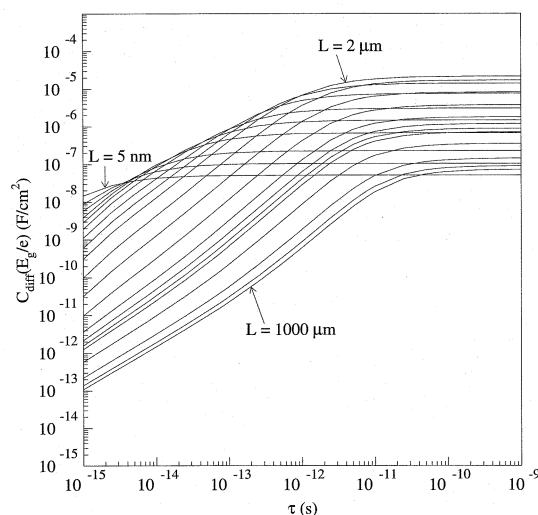


Fig. 4. $C_{\text{diff}}(E_g/e)$ as a function of τ for 20 values of L ranging from 5 nm to $1000 \mu\text{m}$. The values of τ around and below 10^{-14} s are not realistic, but they are included to make the shape and origin of the plotted curves clearer.

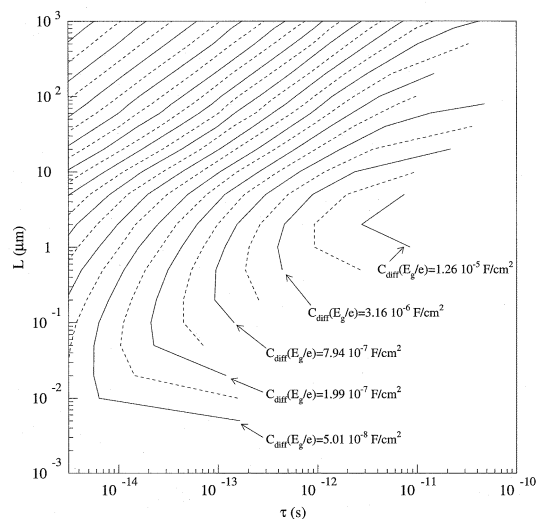


Fig. 5. Iso-capacitance plot showing which combinations of (L, τ) result in the same $C_{\text{diff}}(E_g/e)$. The values of the $C_{\text{diff}}(E_g/e)$ presented range from $1.26 \cdot 10^{-5}$ to $7.94 \cdot 10^{-13}$ F/cm². The ratio of values of $C_{\text{diff}}(E_g/e)$ for any two consecutive iso-curves is $10^{+0.3} \approx 2$. The dashed lines are used for clarity.

Fig. 4 shows that, as the lifetime of the carriers in the active region increases, the $C_{\text{diff}}(E_g/e)$ increases up to a specific lifetime and subsequently becomes constant. This is because the increase of the carrier lifetimes helps minority carriers to reach the contacts. For every value of L there is a specific value of τ for which the maximum of the minority carriers reach the contacts, and further increase of their lifetimes does not contribute to an increase in the diffusion capacitance. The value of τ at which this happens is naturally lower for physically shorter diodes, because the minority carriers have to travel a smaller distance.

It is interesting to plot the iso-curves of the L and τ combinations that result in the same $C_{\text{diff}}(E_g/e)$. This is shown in Fig. 5. The lowest value of $C_{\text{diff}}(E_g/e)$ shown in the plot is $7.94 \cdot 10^{-13}$, the maximum is $1.26 \cdot 10^{-5}$ F/cm², and the capacitance ratio for any two consecutive iso-curves is $10^{+0.3} \approx 2$. This iso-plot is useful for the classification of diodes as long or short, based on their diffusion capacitance.

As already mentioned, the diffusion capacitance is a critical factor for the bandwidth of diodes, with the exception of laser diodes that are

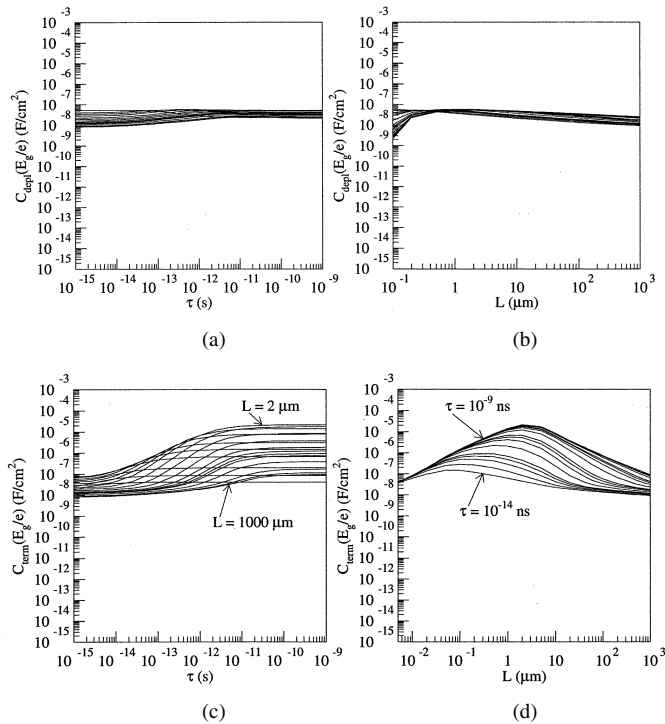


Fig. 6. Depletion capacitance [plots (a) and (b)] and the total terminal capacitance [plots (c) and (d)] at forward bias equal to E_g/e as a function of the half-length of the diode [plots (b) and (d)] and as a function of the lifetime of the carriers in the laser active region [plots (a) and (c)]. We see that the depletion capacitance does not change much with the variation of L and τ and the variations in the terminal capacitance are due to the diffusion capacitance for the corresponding (L, τ) combinations.

physically very long and that have extremely low τ . These laser diodes have a minimal diffusion capacitance, and the depletion capacitance is dominant. To obtain a more quantitative understanding of these limits, we plot the depletion capacitance and the terminal capacitance (sum of the diffusion and depletion capacitances) for a typical bias of laser diodes as a function of L and τ (Fig. 6).⁴ We note that the depletion capacitance is not influenced too much by L and τ , and by varying these variables, we affect mainly the diffusion capacitance. By comparing Figs. 3 and 4 with Fig. 6, we conclude that the diffusion capacitance affects the terminal capacitance and speed of the diode for $\tau > 10^{-11}$ s if $L = 1$ mm and for $\tau > 10^{-14}$ s if $L = 0.02$ μm . Outside this region, manipulating the L and τ for minimizing the diffusion capacitance does not further affect the bandwidth of the diode, as the diffusion capacitance is already very low.

III. CONCLUSION

It is traditionally assumed that the bandwidth of diodes is determined mainly by the minority carrier lifetime. We have shown here by numerical simulation that there is a complex interplay between the physical length and the lifetime, and only both quantities together determine the diffusion capacitance and diode bandwidth.

We have simulated a generic diode with lower lifetime τ of the charge carriers in a short central region (5 nm around the junction) corresponding to the active region of a laser diode. At a typical forward bias of (E_g/e) the diffusion capacitance of the diode is typically larger

⁴We plot the depletion capacitance for $L > 0.1$ μm , as the diodes are depleted for lower L .

than the depletion capacitance, with the exception of very low τ , where the diffusion capacitance is extremely small.

It is shown that for short L , $C_{\text{diff}}(E_g/e)$ increases with L , as the increase of the diffused charge is the dominant effect, whereas for longer L the effect of carrier recombination prevails and the $C_{\text{diff}}(E_g/e)$ falls as a function of L . For very low values of τ , the latter effect is the most important one. It is also shown that $C_{\text{diff}}(E_g/e)$ increases with τ up to a specific value of the lifetime, and then becomes constant, as all the diffused carriers reach the contacts. The value of τ that this occurs is lower for the physically shorter diodes. Finally we have presented the iso- $C_{\text{diff}}(E_g/e)$ curves in the (L, τ) space to explicitly show which combinations of L and τ result in the same diffusion capacitance for a given operational point and equally affect the speed of the diode, for non trivial values of the diffusion capacitance. This plot may prove useful for the design of high bandwidth.

REFERENCES

- [1] K. Hess, *Advanced Theory of Semiconductor Devices*. New York: Wiley, 2000.
- [2] S. E. Laux and K. Hess, "Revisiting the analytical theory of p-n junction impedance: Improvements guided by computer simulation leading to a new equivalent circuit," *IEEE Trans. Electron Devices*, vol. 46, pp. 396–412, Feb. 1999.
- [3] P. Bhattacharya, *Semiconductor Optoelectronic Devices*. Englewood Cliffs: Prentice-Hall, 1994.
- [4] Y. Liu, W.-C. Ng, F. Oyafuso, B. Klein, and K. Hess, "Simulating the modulation response of VCSELs: The effects of diffusion capacitance and spatial hole-burning," *Proc. Inst. Elect. Eng. Optoelectron.*, vol. 149, no. 4, pp. 182–188, Aug. 2002.
- [5] J. Strogas, "Study of the Diffusion Capacitance in Laser Diodes," M.S. thesis, Univ. Illinois, Urbana-Champaign, 2002.
- [6] *Programs MDRAW, DESSIS, and TECPLOT of the ISE-TCAD Package, ISE 6.1/7.5 USER Manuals*, Integrated Systems Engineering, Inc., San Jose, CA.

Avalanche Photodiode-Based Active Pixel Imager

G. F. Marshall, J. C. Jackson, J. Denton, P. K. Hurley, O. Braddell, and A. Mathewson

Abstract—In this brief, an integrated avalanche photodiode–active pixel sensor (APD–APS) for “daylight to subtwilight” imaging has been demonstrated. Excellent logarithmic response of the APS was demonstrated by images taken with a 64×64 pixel array. Image degradation occurred when the APD was operated in sub-Geiger avalanche mode. Analysis of the APD current revealed that leakage from parasitic diodes obscured the internal avalanche gain. The parasitics will be shown to impede fabricating of useful APD–APS circuits and advanced isolation techniques must be employed to operate in avalanche mode.

Index Terms—Avalanche photodiodes (APDs), photodiodes, smart pixels, image sensors, subtwilight imaging.

Manuscript received December 10, 2003. This work was supported in part by funding from the U.K. Ministry of Defence Corporate Research Program. The review of this brief was arranged by Editor J. Hynecek.

G. F. Marshall and J. Denton are with QinetiQ, Malvern, U.K. (e-mail: gf_marshall@qinetiq.com).

J. C. Jackson is with Photon Detection Systems, Ltd., Dublin, Ireland (e-mail: carljackson@photonetection.com).

P. K. Hurley, O. Braddell, and A. Mathewson are with the National Microelectronics Research Centre, Cork, Ireland (e-mail: amathews@nmrc.ie).

Digital Object Identifier 10.1109/TED.2003.823051